Broiler FCR Optimization using Norm Optimal Terminal Iterative Learning Control

Johansen, Simon Vestergaard; Riisgaard Jensen, Martin; Chu, Bing; Bendtsen, Jan Dimon; Mogensen, Jesper; Rogers, Eric

Published in:
I E E E Transactions on Control Systems Technology

DOI (link to publication from Publisher):
10.1109/TCST.2019.2954300

Publication date:
2021

This article has been accepted for inclusion in a future issue of this journal. Content is final as presented, with the exception of pagination.

Broiler FCR Optimization Using Norm Optimal Terminal Iterative Learning Control

Simon V. Johansen, Martin R. Jensen, Bing Chu, Jan D. Bendtsen, *Member, IEEE*, Jesper Mogensen, and Eric Rogers

***Abstract*— Broiler feed conversion rate (FCR) optimization reduces the amount of feed, water, and electricity required to produce a mature broiler, where temperature control is one of the most influential factors. Iterative learning control (ILC) provides a potential solution given the repeated nature of the production process, as it has been especially developed for systems that make repeated executions of the same finite duration task. Dynamic neural network models provide a basis for control synthesis, as no first-principle mathematical models of the broiler growth process exist. The final FCR at slaughter is one of the primary performance parameters for broiler production, and it is minimized using a modified terminal ILC law in this article. Simulation evaluation of the new designs is undertaken using a heuristic broiler growth model based on the knowledge of a broiler application expert and experimentally on a state-of-the-art broiler house that produces approximately 40 000 broilers per batch.**

***Index Terms*— Biosystems, iterative learning control (ILC), neural networks.**

I. Introduction

The global demand for poultry meat is predicted to increase by 18% between 2015–2017 and 2027 to 139 billion kg [1, p. 37], of which broiler (i.e., a chicken that is bred and raised specifically for meat production) meat will represent the majority. Industrial state-of-the-art broiler production typically has 30–40 000 broilers per batch, produces 2050-g broilers in 34 days from 42-g newly hatched broilers, and employs ad libitum feeding and drinking strategies, i.e., unrestricted access to feed and water. Broiler feed conversion rate (FCR) optimization reduces the amount of feed, water, and electricity required to produce a mature broiler.

Tight bounds on the production environment must be met to enable optimal growth, which requires manual tuning of each broiler house by a broiler application expert. Active feed control is not practically feasible in the state-of-the-art broiler production as ad libitum feeding regimes are used. Temperature control is, however, highly influential and practically feasible.

Broiler production is mature in terms of data acquisition due to tight biosecurity and traceability requirements. This, in turn, drives the need to automatically optimize performance in a data-driven framework by suitably designed temperature control. In this article, a design based on combining iterative learning control (ILC) and dynamic neural network (DNN) modeling is developed and evaluated in both simulation and implementation in a state-of-the-art broiler house.

The development of ILC was motivated by many processes that repeat the same finite duration task over and over again, e.g., a gantry robot undertaking a "pick and place" task. Each execution is commonly termed a trial or pass and the finite duration is known as the pass or trial length. Once a trial is completed, the system resets to the starting location and the next trial can begin, exactly as in broiler production. Moreover, all data recorded during the previous trial are available for use in computing the control input for the next trial with the overall aim of improving performance from trial-to-trial.

The survey articles [2] and [3] are a good starting point for the ILC literature. The scope of ILC laws in the literature ranges from simple structure laws, such as phase-lead, that can be tuned without the use of a model through to advanced model-based designs for linear and nonlinear dynamics. Mature ILC application areas with experimental validation include additive manufacturing (see [4]) and an extension to robotic-assisted stroke rehabilitation for the upper limb with supporting clinical trials [5].

Model-based ILC is required for broiler FCR optimization since the broiler growth process itself is highly nonlinear and time-varying (see Fig. 1 for a schematic of the inputs, outputs, and disturbances that are relevant to the application of control laws to the broiler process). This article uses nonlinear data-driven modeling in the form of DNNs to model the dynamic relationship between the climate conditions and the broiler growth (see [6] for background information on neural networks). Such models have been successfully applied to model complex biological processes, of which noncontrol-related applications include broiler growth forecasting [7], [8].

This article gives the first results on a new application of ILC to food production. In particular, ILC is modified

Manuscript received October 4, 2019; accepted October 22, 2019. Manuscript received in final form November 14, 2019. This work was supported by Innovationsfonden under Grant 5016-00133B. Recommended by Associate Editor K. Barton. *(Corresponding author: Simon V. Johansen.)*

S. V. Johansen is with SKOV A/S, 7870 Roslev, Denmark, and also with the Department of Electronic Systems, Aalborg University, 9100 Aalborg, Denmark (e-mail: sjo@skov.dk).

M. R. Jensen and J. Mogensen are with SKOV A/S, 7870 Roslev, Denmark (e-mail: mri@skov.dk; jmo@skov.dk).

B. Chu and E. Rogers are with the School of Electronics and Computer Science, University of Southampton, Southampton SO14 0DA, U.K. (e-mail: b.chu@soton.ac.uk; etar@soton.ac.uk).

J. D. Bendtsen is with the Department of Electronic Systems, Aalborg University, 9100 Aalborg, Denmark (e-mail: dimon@es.aau.dk).

Color versions of one or more of the figures in this article are available online at http://ieeexplore.ieee.org.

Digital Object Identifier 10.1109/TCST.2019.2954300

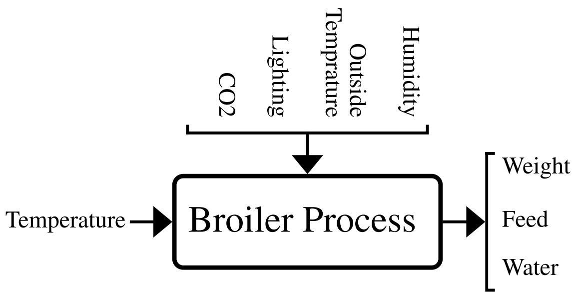

Fig. 1. Overview of the broiler process in terms of inputs (left), disturbances (top), and outputs (right).

to minimize the terminal broiler FCR in the presence of the uncertain nature of the data-driven DNN model. To evaluate the new design in simulation, a heuristic broiler growth model is developed based on the experience and knowledge of a broiler application expert, which is then analyzed to provide FCR optimization guidelines. In [9], the preliminary ILC law design and associated simulation study of a heuristic broiler growth model were reported. The results in this article differ substantially by including cumulative feed consumption output in the heuristic model, measurement weight bias compensation as investigated in [10], and experimental results from a state-of-the-art broiler production facility.

This article is organized as follows. The development of a heuristic broiler model and the broiler FCR minimization problem is described in Section II. Terminal ILC is then introduced and applied to solve the FCR minimization problem in Section III. A simulation study of the design is given in Section IV followed by the experimental results in Section V. Finally, Section VI gives the conclusions and briefly discusses possible future research.

Notation: Let $u_k[n] \in \mathbb{R}^{N_u}$ be a signal at trial k and sample n, and U_k be the supervector formed from $u_k[n]$ in the finite-time interval between the first sample N_s and last sample N_e as

$$U_k = [u_k[N_s]^T \quad \cdots \quad u_k[N_e]^T]^T \in \mathbb{R}^{N_u N_n} \tag{1}$$

with a total of $N_n = N_e - N_s + 1$ samples; $\tilde{U}_k = u_k[N_e]$ is the terminal supervector. Let a be a vector and A be a positive-definite matrix, and then, $\|a\| = a^T a^{1/2}$ is the Euclidean norm of a and $\|a\|_A = a^T A a^{1/2}$ is the weighted Euclidean norm of a. Let B and C be sets, and then, $\#B$ is the cardinality of B and $B \backslash C = \{x \in B \mid x \notin C\}$ is the difference of B and C.

II. Heuristic Broiler Growth Model and FCR Optimization

A. Heuristic Broiler Growth Model

The heuristic broiler FCR model developed in this section is used to test the data-driven broiler growth optimization algorithm developed in Section III-C in a simulation environment prior to experimental tests. Only past growth model data, and not the growth model, is used for control synthesis, which would also be the case under real production conditions. The objective is to represent basic broiler growth behavior in an industrial state-of-the-art broiler production, which is based on the experience and knowledge of a broiler application expert.

The model's primary objective is to assess the algorithm's ability to iteratively learn a unique time series of broiler state-dependent temperature inputs that minimize the terminal broiler FCR while simulating reduced growth for both negatively and positively suboptimal temperature inputs. Such a broiler growth model can be represented by the discrete-time dynamic nonlinear model

$$\begin{bmatrix} x_m[n+1] \\ x_f[n+1] \end{bmatrix} = \begin{bmatrix} x_m[n] \\ x_f[n] \end{bmatrix} + T_s \begin{bmatrix} G(u[n],\, x_m[n]) \\ R_f(x_m[n]) \end{bmatrix} \tag{2a}$$

$$\begin{bmatrix} y_w[n] \\ y_f[n] \end{bmatrix} = \begin{bmatrix} R_w(x_m[n]) \\ x_f[n] \end{bmatrix} + \begin{bmatrix} q_w[n] + q_{w,\text{bias}}[n] \\ q_f[n] \end{bmatrix} \tag{2b}$$

$$\Gamma = R_w(x_m[N_e]) \tag{2c}$$

with initial conditions $x_m[N_s] = x_f[N_s] = 0$ and measured slaughter weight $\Gamma \in \mathbb{R}$, where $x_m[n] \in \mathbb{R}_+$ is the broiler maturity in "effective growth days," $y_w[n] \in \mathbb{R}_+$ is the measured broiler weight, $x_f[n] \in \mathbb{R}_+$ is the cumulative feed consumption, $y_f[n] \in \mathbb{R}_+$ is the measured cumulative feed consumption, $u[n] \in \mathbb{R}$ is the temperature input, and $T_s \in \mathbb{R}_+$ is the sampling interval in days. Under production conditions, the temperature input $u[n]$ is a reference for the climate control system, which, for simplicity, is assumed to achieve perfect tracking. In (2a), G is a function representing the broiler growth rate, while $R_w \colon \mathbb{R}_+ \to \mathbb{R}_+$ and $R_f \colon \mathbb{R}_+ \to \mathbb{R}_+$ are smooth and strictly increasing functions mapping the broiler maturity $x_m[n]$ into broiler weight and feed consumption, $q_w[n] \in \mathbb{R}$ is the weight measurement noise, $q_{w,\text{bias}}[n] \in \mathbb{R}$ is the weight bias, and $q_f[n] \in \mathbb{R}$ is the feed measurement noise.

The growth and feed consumption of the widely used ROSS 308 fast growing broiler strain are described by the manufacturer in [12, p. 3] as

$$R_w(t) = \frac{-18.3\,t^3 + 2.2551\,t^2 + 2.9118\,t + 54.739}{1000} \tag{3a}$$

$$R_f(t) = \frac{21.9 \cdot 10^{-6}\,t^4 - 4.232 \cdot 10^{-3}\,t^3 + 0.206\,t^2}{1000} + \frac{2.02\,t + 11.6}{1000} \tag{3b}$$

where $R_w(t) \in \mathbb{R}_+$ is the broiler weight reference in kg, $R_f(t) \in \mathbb{R}_+$ is the broiler feed uptake reference in kg/day, and $t \in [0, 59]$ days is the time in "effective growth days." Expressing broiler weight $R_w(x_m[n])$ and broiler feed uptake $R_f(x_m[n])$ in terms of the broiler maturity in "effective growth days" through $x_m[n]$ results in realistic weight and feed uptake behavior, as it captures the nonlinear nature of broiler growth. The polynomials are determined by the manufacturer using statistical means.

The maturation rate function $G \colon \mathbb{R} \times \mathbb{R}_+ \to [\beta, 1]$, where $\beta \in [0, 1[$ is a worst case broiler growth rate, represents the influence of external stimuli u on the broilers' relative maturation. It keeps track of the metabolized energy, as shown in Fig. 2. It is not possible to construct this function from "first principles"; instead, a broiler application expert will heuristically specify the decreased growth rate for a specific temperature deviation from "optimal" growth conditions.

This article has been accepted for inclusion in a future issue of this journal. Content is final as presented, with the exception of pagination.

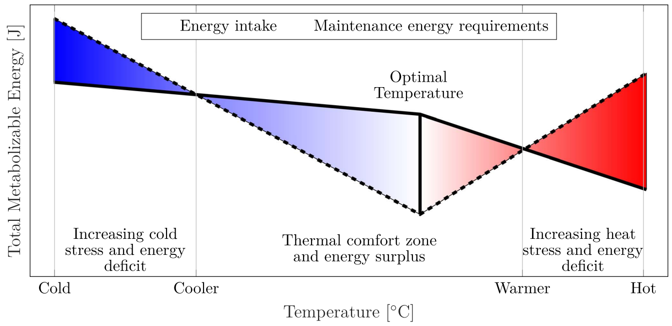

Fig. 2. Total metabolized energy for different temperature categories in terms of energy intake and maintenance energy requirements. Blue denotes a cold temperature, red denotes hot temperature, and white denotes thermoneutral temperature. The optimal temperature is marked with a vertical line [11, p. 4].

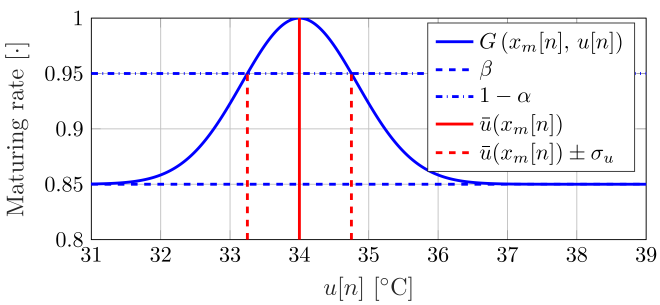

Fig. 3. Visualization of the maturation rate function $G(x_m[n], u[n])$ for $x_m[n] = 0$ with worst case broiler growth rate $\beta = 0.85$ and $\alpha = 0.05$, maximizing input $\bar{u}(x_m[n]) = 34$ [°C] and temperature error sensitivity $\sigma_u = 0.75$ [°C].

In this article, a modified normal distribution is chosen for G, as it has a unique maximum and the standard deviation can easily be tuned to design how sensitive G is to temperature errors. Specifically

$$
\begin{aligned}
&G(u[n], x_m[n]) \\
&= \beta + (1-\beta)\exp\left\{\ln\left(\frac{\alpha+\beta-1}{\beta-1}\right)\left[\frac{u[n]-\bar{u}(x_m[n])}{\sigma_u}\right]^2\right\}
\end{aligned} \tag{4}
$$

where $\bar{u}(x_m[n])$ is the temperature maximizing G, $G(\bar{u}(x_m[n]), x_m[n]) = 1$, and $\sigma_u \in \mathbb{R}_+$ is the constant temperature sensitivity. The temperature sensitivity is the temperature input error, $u[n] - \bar{u}(x_m[n])$, resulting in a decreased maturation rate of α—-corresponding to $G(\bar{u}(x_m[n]) \pm \sigma_u, x_m[n]) = 1 - \alpha$ with $\alpha \in]0, 1-\beta[$.

The parameters of the maturation rate function G are shown in Fig. 3. For a more accurate temperature sensitivity, the broilers' feathering and ability to regulate their own body temperature could also be considered, but this could make σ_u time and state dependent and is left as a subject for possible future research.

The optimal temperature profile is unknown in the industry, but typical temperature profiles for the ROSS 308 fast growing broiler transition almost linearly between the initial temperature of $\bar{u}_s = 34$ °C at day $t_s = 0$ to $\bar{u}_e = 21$ °C at day $t_e = 34$. This corresponds to a temperature drop of $(\bar{u}_e - \bar{u}_s)$, which is modeled as proportional to the maturity $x_m[n]$ as

$$\bar{u}(x_m[n]) = \bar{u}_s + \Delta T x_m[n] \quad \text{with } \Delta T = \frac{\bar{u}_e - \bar{u}_s}{t_e - t_s}. \tag{5}$$

Consequently, the optimal temperature at sample n depends on $x_m[n-1]$, which, in turn, depends on all prior inputs.

The weight bias term $q_{w,\text{bias}}[n]$ was investigated in [10] and found to cause terminal weight measurement errors, with -27.4-g mean and 115.9-g standard deviation through comparison with the accurately measured slaughter weight. This problem was first reported in [13] but has subsequently received limited research attention. In [14], it was observed that the automatic weighting system was used less frequently by heavier broilers through image analysis and subsequently confirmed in [15]. The weight bias onset was found to occur around day 15 in [10], which is heuristically assumed to increase linearly from zero at day 15 to $\mathcal{Q}_{\text{bias}} \sim \mathcal{N}(-27.4 \text{ g}, 115.9 \text{ g})$ at the terminal sample and hence

$$y_{w,\text{bias}}[n] = \begin{cases} \dfrac{nT_s - 15}{N_e T_s - 15}\mathcal{Q}_{\text{bias}}, & 15 < nT_s \\ 0, & \text{otherwise} \end{cases} \tag{6}$$

where $\mathcal{Q}_{\text{bias}}$ is constant throughout each simulation, as shown in Fig. 4(a). In [10], it was found that using the measured slaughter weight, i.e., the terminal broiler weight, reduces the weight bias effect for broiler weight prediction on real broiler production data.

The noise terms $q_w[n]$ and $q_f[n]$ are found by analyzing the frequency spectrum of production data from the experimental test site. As broiler weight is a smooth function of time, the "true" broiler weight is approximated by a second-order polynomial $\hat{y}_{w,\text{pol},2}$ between days 3 and 15, where the weight measurement y_w is expected to be the most reliable. The fit errors, $y_w - \hat{y}_{w,\text{pol},2}$, of 36 batches from the experimental test site are shown in the top plot of Fig. 4(b) and are treated as measurement noise. Note that it is not feasible to evaluate the performance of this noise model.

Subtracting the mean, concatenating all the fit errors, and computing the FFT produces the bottom magnitude plot. As this is not a standard distribution, random realizations of $q_w[n]$ with identical magnitude are obtained by randomly rotating the phases of the FFT and applying the inverse discrete Fourier transform. For more information on this approach, see [16]. Some realizations of $q_w[n]$ are shown in the top plot of Fig. 4(b). Similarly, the "true" cumulative feed uptake is approximated by a fourth-order polynomial $\hat{y}_{f,\text{pol},4}$ between days 3 and 30 and shown in Fig. 4(c) (using the same order of polynomial fit as proposed by the ROSS 308 manufacturer).

B. Control Design Considerations

Potential broiler production optimization strategies are discussed in this section. They consist of weight maximization, feed minimization, and FCR maximization.

1) Weight Maximization: The objective for this strategy is to maximize $\bar{y}_w[n]$. Inspecting G shows that $x_m[n]$ is maximized by the unique input $\bar{u}(x_m[n])$ that for all $u[n] \neq \bar{u}(x_m[n])$ satisfies

$$G(u[n], x_m[n]) < G(\bar{u}(x_m[n]), x_m[n]) = 1.$$

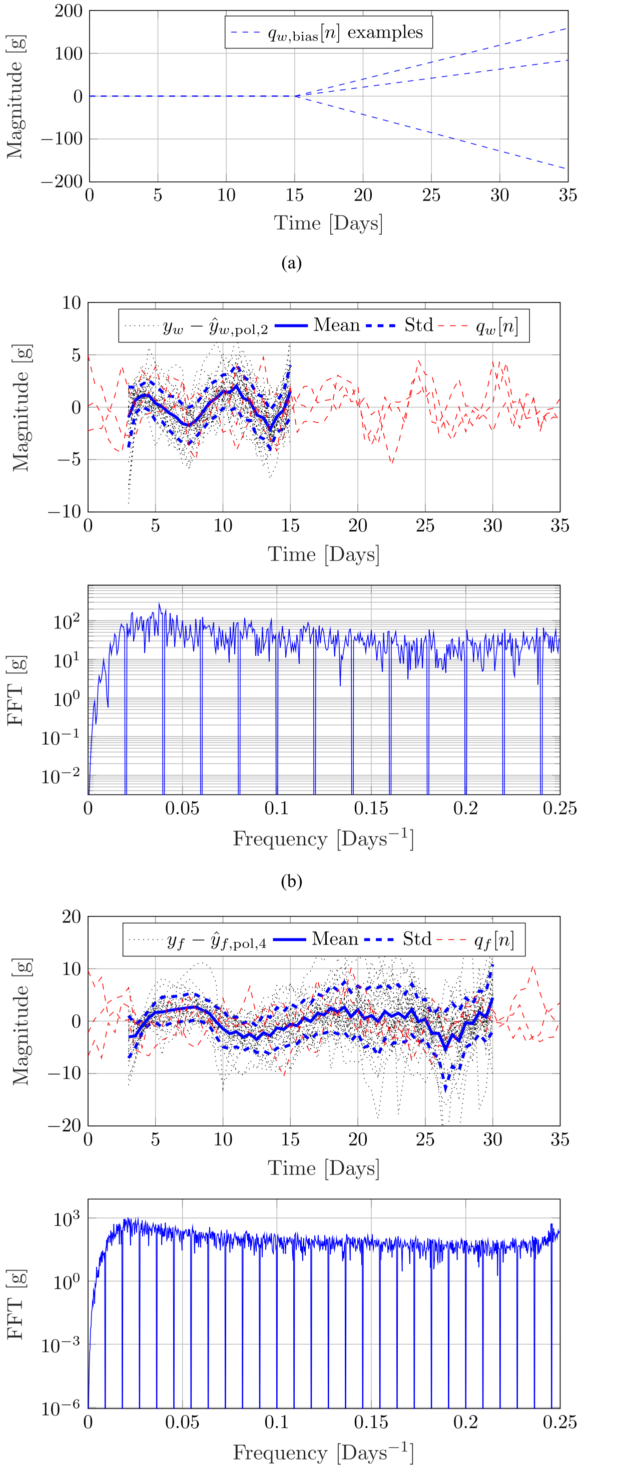

Fig. 4. Measurement behavior for the heuristic broiler growth model. (a) Weight measurement bias $q_{w,\mathrm{bias}}[n]$ samples using (6). (b) Visualization of the weight measurement noise $q_w[n]$. (c) Visualization of the feed uptake measurement noise $q_f[n]$.

In the case when $\beta \leq G \leq 1$, the largest possible maturity $\bar{x}_m[n]$ equals

$$\begin{aligned}\bar{x}_m[n] &= \max\{x_m[n]\}\\ &= T_s \sum_{i=1}^{n} \max\{G(u[i],\, x_m[i])\} = n\,T_s.\end{aligned}$$

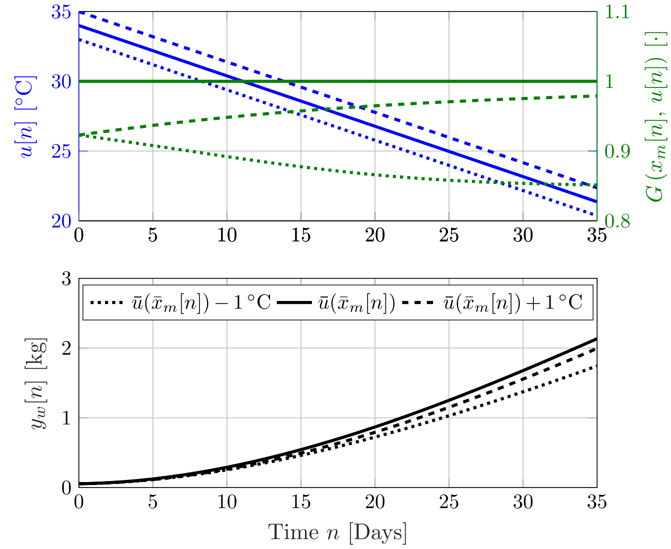

Fig. 5. Visualization of broiler growth y_m with different inputs. The top plot depicts the maturation rate function $G(x_m[n],\, u[n])$ as a function of the input $u[n]$ and the bottom plot depicts the output $y_m[n]$. The model settings equal those of Fig. 3 with $T_s = 1$ day.

As R_w is strictly increasing, the largest possible broiler weight is given by

$$\begin{aligned}\bar{y}_w[n] &= \max\{y_w[n]\} = \max\{R_w(x_m[n])\}\\ &= R_w(\max\{x_m[n]\}) = R_w(n\,T_s).\end{aligned}$$

This ensures that suboptimal control results in suboptimal weight, as expected in real broiler production where either a too low or too high temperature results in decreased broiler growth, as shown in Fig. 2. In Fig. 5, the behavior of the broiler model is shown for different temperature inputs.

2) Feed Minimization: The objective for this strategy is to minimize $\bar{y}_f[n]$. As $\beta \leq G \leq 1$, the smallest maturation rate $\underline{x}_m[n]$ is governed by

$$\begin{aligned}\underline{x}_m[n] &= \min\{x_m[n]\}\\ &= T_s \sum_{i=1}^{n} \min\{G(u[i],\, x_m[i])\} = T_s \beta n. \qquad (7)\end{aligned}$$

As R_f is strictly increasing, the lowest cumulative feed consumption is given by

$$\begin{aligned}\underline{x}_f[n] &= \min\{x_f[n]\} = \min\left\{T_s \sum_{i=1}^{n} R_f(x_m[i])\right\}\\ &= T_s \sum_{i=1}^{n} R_f(\min\{x_m[i]\}) = T_s \sum_{i=1}^{n} R_f(T_s \beta i). \qquad (8)\end{aligned}$$

This suggests that feed minimization and weight maximization are completely opposing goals.

3) FCR Minimization: The expression for FCR from the heuristic model is

$$y_{\mathrm{FCR}}[n] = \frac{y_f[n]}{y_w[n]} = \frac{x_f[n]}{R_w(x_m[n])} = T_s \frac{\sum_{i=1}^{n} R_f(x_m[i])}{R_w(x_m[n])}. \qquad (9)$$

The objective for this strategy is to minimize $y_{\mathrm{FCR}}[n]$. In contrast to weight maximization and feed minimization, an analytical expression for the lowest possible FCR is nontrivial

This article has been accepted for inclusion in a future issue of this journal. Content is final as presented, with the exception of pagination.

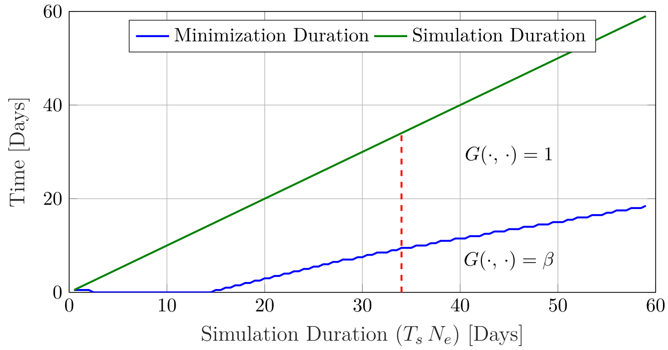

Fig. 6. Minimization duration as a function of simulation duration $(N_e T_s)$ with $\beta = 0.85$ and $T_s = 0.5$ days, which corresponds to the length of the initial period where $G(x_m[n], u[n]) = \beta$. The red dashed line indicates a simulation duration of 34 days with a minimization duration of 9.5 days, equivalent to Fig. 7.

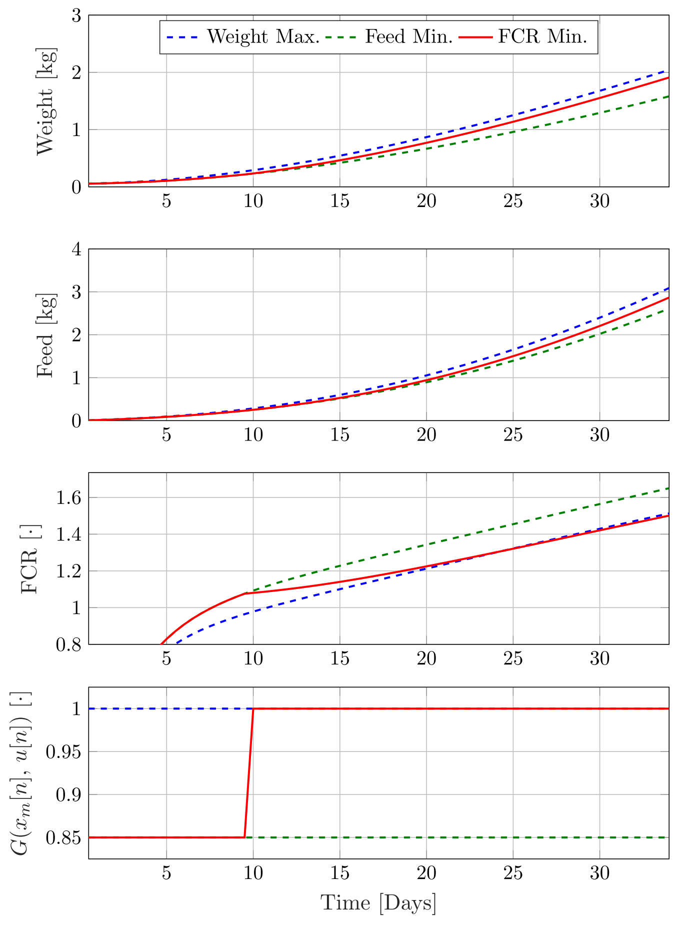

Fig. 7. Visualization of different optimization strategies with $N_e = 34$ days, $T_s = 0.5$ day, and $\beta = 0.85$. An FCR difference of 1.14×10^{-3}, equivalent of 1.1%, exists between growth maximization and FCR minimization, which potentially makes FCR minimization a better strategy.

to determine. This is due to two simultaneous and opposing objectives, namely weight maximization and feed minimization, which depends on the simulation duration N_e, as shown in Fig. 6.

In Fig. 7, the strategies are compared, from which it follows that FCR minimization consists of an initial period of feed minimization followed by weight maximization. Feed minimization produces the highest FCR and is therefore excluded. Moreover, weight maximization results in a 1.1% higher FCR than FCR minimization, which makes FCR minimization favorable despite the added complexity of another output and this objective will, therefore, be used in this article.

III. Broiler FCR Minimization Using Terminal ILC

A. Terminal ILC

Terminal ILC (TILC) is a method that can be applied to a repeating process with the aim of iteratively learning the input sequence $U_k \in \mathbb{R}^{N_u N_n}$ such that the terminal process output $\tilde{Y}_k(U_k) \in \mathbb{R}^{N_y}$ tracks the desired terminal reference $\tilde{R} \in \mathbb{R}^{N_y}$ denoted by

$$\lim_{karrow\infty} \tilde{Y}_k(U_k) = \tilde{R} \tag{10}$$

with the supervector model used for control synthesis given by

$$\tilde{Y}_k(U_k) = \tilde{P}U_k + \tilde{K} \tag{11}$$

where $\tilde{P} \in \mathbb{R}^{N_y \times N_u N_n}$ is the terminal system matrix and $\tilde{K} \in \mathbb{R}^{N_y}$ represents the terminal effects unrelated to the input $U \in \mathbb{R}^{N_u N_n}$.

This last problem can be solved using constrained norm optimal point-to-point ILC, which aims to track the output at specific samples using techniques also discussed in [17] and [18]. As TILC only aims to track the terminal output, TILC is a specialization of point-to-point ILC. Adapting the constrained norm optimal point-to-point ILC algorithm 1 in [18] to the special case of the TILC problem considered gives

$$U_{k+1} = \arg\min_{U\in\Omega} \|\tilde{E}_k(U)\|^2_{W_{\tilde{E}}} + \|U - U_k\|^2_{W_{\Delta U}} \tag{12a}$$

$$\text{s.t. } \tilde{E}_k(U) = \tilde{R} - \tilde{Y}_k(U) \text{ and} \tag{12b}$$

$$\tilde{Y}_k(U) = \tilde{P}U + \tilde{K} \tag{12c}$$

where Ω is the set of valid inputs, $W_{\tilde{E}} \in \mathbb{R}^{N_y \times N_y}$ is the symmetric positive definite tracking error cost matrix, $W_{\Delta U} \in \mathbb{R}^{N_u N_n \times N_u N_n}$ is the symmetric positive definite input change cost matrix, and $\tilde{E}_k(U) \in \mathbb{R}^{N_y}$ is the terminal tracking error given by (12b). The intuition behind (12) is to reduce the terminal tracking error by finding an input in the neighborhood of U_k that minimizes the cost function (12a).

The following results were established in [18] and are repeated here for convenience since they encapsulate the aim of the control design under ideal conditions.

Theorem 1: If perfect tracking is feasible, i.e., $\exists\ U \in \Omega$ such that $\tilde{Y}_k(U) = \tilde{R}$, then (12) achieves monotonic convergence to zero tracking error

$$\|\tilde{E}_{k+1}(U_{k+1})\|_{W_{\tilde{E}}} \le \|\tilde{E}_k(U_k)\|_{W_{\tilde{E}}} \quad \forall k \in \mathbb{Z}_+ \tag{13}$$

and

$$\lim_{k\to\infty} \tilde{E}_k(U_k) = 0, \quad \lim_{k\to\infty} U_k = \bar{U}. \tag{14}$$

This article has been accepted for inclusion in a future issue of this journal. Content is final as presented, with the exception of pagination.

Theorem 2: If perfect tracking is not feasible, i.e., $\tilde{Y}_k(U) \neq \tilde{R} \quad \forall U \in \Omega$, then the input of (12) converges to

$$= \arg\min_{U \in \Omega} \|\tilde{R} - \tilde{P}U - \tilde{K}\|^2_{W_{\tilde{E}}} \tag{15}$$

equivalent to the algorithm converging to the smallest possible tracking error. Moreover, this convergence is monotonic in the tracking error norm

$$\|\tilde{E}_{k+1}(U_{k+1})\|_{W_{\tilde{E}}} \leq \|\tilde{E}_k(U_k)\|_{W_{\tilde{E}}} \quad \forall k \in \mathbb{Z}_+. \tag{16}$$

B. Data-Driven Model

This section provides an overview of the model (see [8], [10] for a detailed description).

The objective of the data-driven model is to enable control synthesis without a mathematical broiler FCR model, by synthesizing $\tilde{P}$ and $\tilde{K}$ from (12c) using past production data. Using a nonlinear discrete-time data-driven model, the aim is to capture the broiler growth dynamic using data from the past N_b trials $\{\{U_{k-N_b+1}, D_{k-N_b+1}, Y_{k-N_b+1}\}, \ldots, \{U_k, D_k, Y_k\}\}$, where D_k denotes the disturbance vector and N_b data indexes are conveniently denoted by

$$\mathcal{B}_k = \{k - N_b + 1, \ldots, k\}. \tag{17}$$

For data-driven model synthesis at trial k, data from the trial indexes denoted by $\mathcal{B}_{k-1}$ are required. Trial data prior to the first trial, $k<1$, are denoted as preliminary trials, e.g., $\{U_{-2}, D_{-2}, Y_{-2}\}$. Hence, a total of N_b preliminary trials are required for model synthesis for the first trial, $k = 1$, denoted by the indexes $\mathcal{B}_0 = \{1 - N_b, \ldots, 0\}$.

The data-driven model is chosen to be a nonlinear autoregressive moving average model with exogenous input (NARMAX)-type model implemented as a neural network with N_l input and output lags, a single hidden layer with N_N neurons, and a hyperbolic tangent activation function in the hidden layer

$$\hat{y}_k[n+1 \mid \mathcal{W}, s] = W^{\mathrm{o}} \tanh(\mathcal{X} + \theta^{\mathrm{h}}) + \theta^{\mathrm{o}} \tag{18}$$

with

$$\mathcal{X} = \sum_{i=0}^{N_l-1} W^{\mathrm{h}}_{y,i}\hat{y}_k[n-i \mid \mathcal{W}, s] + W^{\mathrm{h}}_{u,i}u_k[n-i] + W^{\mathrm{h}}_{d,i}d_k[n-i]$$

where $W^{\mathrm{o}} \in \mathbb{R}^{N_y \times N_N}$, $\mathcal{X} \in \mathbb{R}^{N_N}$, $\theta^{\mathrm{o}} \in \mathbb{R}^{N_N}$, $W^{\mathrm{h}}_{y,i} \in \mathbb{R}^{N_N \times N_y}$, $W^{\mathrm{h}}_{u,i} \in \mathbb{R}^{N_N \times N_u}$, $W^{\mathrm{h}}_{d,i} \in \mathbb{R}^{N_N \times N_d}$, $\theta^{\mathrm{h}} \in \mathbb{R}^{N_N}$ are model parameters stored in $\mathcal{W}$, and $\hat{y}_k[n \mid \mathcal{W}, s]$ is the model output at sample n, initialized at sample s with model weights $\mathcal{W} \in \mathbb{R}^{N_W}$. Initialization in this case is described by

$$\hat{y}_k[n \mid \mathcal{W}, s] = y_k[n] \quad \forall n \leq s \tag{19}$$

where n is implicitly lower bounded by the starting sample N_s, $N_s \leq n$, for $y_k[n]$, $u_k[n]$, and $d_k[n]$.

To find the model weights, the following training procedure was used:

$$\mathcal{W}(B) = \arg\min_{\mathcal{W}} \sum_{b \in B \setminus \min\{B\}} \frac{J_b(\mathcal{W})}{\#B - 1} \tag{20a}$$

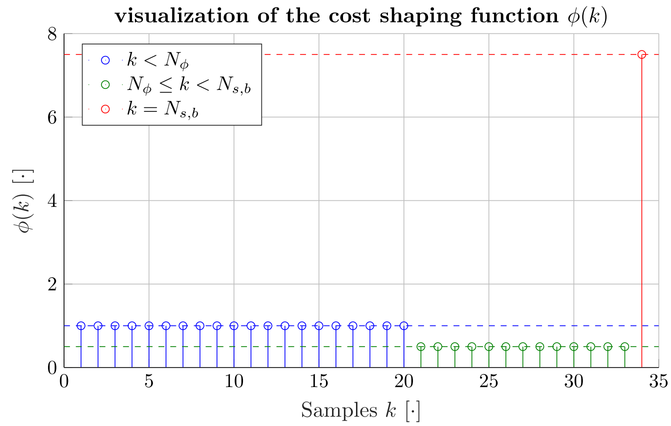

Fig. 8. Visualization of the cost shaping function $\phi(k)$ with $N_\phi = 20$, $N_{s,b} = 34$, and $\gamma = 0.5$. The blue, green, and red values correspond to a separate case of (20d).

with

$$J_b(\mathcal{W}) = \bar{\alpha}\|\mathcal{W}\|^2 + \sum_{i=1}^{N_S}\sum_{n=S_i}^{N_e} \frac{\mathcal{E}_b}{N_y(N_e - S_i + 1)} \tag{20b}$$

$$\mathcal{E}_b = \sum_{i=1}^{N_y} \begin{cases} ||\Gamma_b - \hat{y}_i||_2^2\,\phi(k), & k = N_{s,b} \wedge i = i_w \\ ||y_i - \hat{y}_i||_2^2\,\phi(k), & k \neq N_{s,b} \wedge i = i_w \\ ||y_i - \hat{y}_i||_2^2, & \text{otherwise} \end{cases} \tag{20c}$$

$$\phi(k) = \begin{cases} 1, & k < N_\phi \\ 1 + (N_{s,b} - N_\phi)(\gamma - 1), & k = N_{s,b} \\ \gamma, & \text{otherwise} \end{cases} \tag{20d}$$

where B is a set of batch indices used for training, $S = \{S_1, \ldots, S_{N_S}\}$ is the set of $N_S \in \mathbb{Z}_+$ initialization locations, which was found to speed up training as described in [8], Γ_b is the broiler slaughter weight of batch b, i.e., the true broiler weight prior to slaughter, $i_w \in \mathbb{Z}$ is the weight output index, $\phi\colon \mathbb{Z}_+ \to \mathbb{R}$ is the weight cost shaping function, $N_\phi \in \mathbb{Z}$ is the start weight cost shaping sample number, and $\gamma \in]0, 1[$ is the weight cost shaping parameter.

Automatic weighing pads are commonly used for weighing broilers and are known to be negatively biased onward from day 15, which is represented by (6) in the heuristic model. In [10], the weight cost shaping function $\phi\colon \mathbb{Z}_+ \to \mathbb{R}$ in (20c) and (20d) was found to decrease the impact of this bias—one example of ϕ is shown in Fig. 8. The slaughter weight is considered very accurate and is included by overriding the last measured local weight at sample $k = N_{s,b}$ of each batch. Extra emphasis is then placed on the slaughter weight at sample $k = N_{s,b}$ in the cost function, while samples beyond $N_\phi \in \mathbb{Z}_+$ are weighted less.

The cost function is minimized using the Levenberg–Marquardt algorithm with early stopping applied on the oldest batch index in B, denoted by $\min\{B\}$, in $J_{\min\{B\}}(\mathcal{W})$, to prevent overtraining. The regularization constant $\bar{\alpha} \in \mathbb{R}_+$ is found iteratively through Bayesian regularization to prevent overfitting. The model weights $\mathcal{W}$ are initialized using the Nguyen–Widrow initialization scheme. For detailed information regarding the training, see [8] and [10].

As (20a) is not a convex optimization problem, the weights $\mathcal{W}(B)$ are not guaranteed to be the global minimum. To decrease the probability of finishing in a local minimum, the ensemble mean of N_m models trained with different initial model weights is used. The ensemble data-driven model simulated from sample N_s with data from batch b, $\{Y_b, D_b, U_b\}$, is

$$\hat{y}_{k,b}[n] = \frac{1}{N_m}\sum_{l=1}^{N_m} \hat{y}_b[n \mid \mathcal{W}_l(\mathcal{B}_k \backslash b), N_s] \tag{21}$$

where $\mathcal{W}_l(\mathcal{B}_k\backslash b)$ is the lth training of $\mathcal{W}(\mathcal{B}_k\backslash b)$ with the batch indexes $\mathcal{B}_k\backslash b$ to separate training data and simulation data. The terminal supervector ensemble data-driven model required for (12) is obtained by linearizing (21) along the trajectory of U_b (a past trial) using the first-order Taylor expansion

$$\tilde{Y}_k(U) \approx \hat{\tilde{Y}}_{k,b} + \hat{\tilde{P}}_{k,b}(U - U_b) = \hat{\tilde{P}}_{k,b}U + \hat{\tilde{K}}_{k,b} \tag{22}$$

with

$$\hat{\tilde{P}}_{k,b} = \left.\frac{d\hat{\tilde{Y}}_{k,b}}{dU_b^T}\right|_{U_b} \quad \text{and } \hat{\tilde{K}}_{k,b} = \hat{\tilde{Y}}_{k,b}(U_b) - \hat{\tilde{P}}_{k,b}U_b$$

where $U \in \mathbb{R}^{N_u N_n}$ is the supervector input used in (12c) and U_k is the input for the current trial. The data-driven model is retrained for every k and b (see [19] for detailed derivations of $\hat{\tilde{P}}_{k,b}$ and $\hat{\tilde{K}}_{k,b}$).

Using this model for FCR minimization requires an augmented data-driven model, denoted by $(\cdot)^*$. This model is given by

$$\tilde{Y}_k^*(U) = \frac{\tilde{Y}_{k,f}(U)}{\tilde{Y}_{k,w}(U)} \tag{23}$$

where $\tilde{Y}_{k,w}(U) \in \mathbb{R}_+$ and $\tilde{Y}_{k,f}(U) \in \mathbb{R}_+$, respectively, denote the weight and cumulative feed uptake—the equivalent of (2b). Linearizing in U_b by a first-order Taylor expression similar to (22) results in

$$\tilde{Y}_k^*(U) \approx \hat{\tilde{Y}}_{k,b}^*(U_k) + \hat{\tilde{P}}_{k,b}^*(U - U_k) = \hat{\tilde{P}}_{k,b}^*U + K_{k,b}^* \tag{24}$$

with

$$\hat{\tilde{P}}_{k,b}^* = \frac{d\hat{\tilde{Y}}_{k,b}^*(U)}{d\hat{\tilde{Y}}_{k,b}^T(U)}\frac{d\hat{\tilde{Y}}_{k,b}(U)}{dU^T} = \frac{d\hat{\tilde{Y}}_{k,b}^*(U)}{d\hat{\tilde{Y}}_{k,b}^T(U)}\hat{\tilde{P}}_{k,b}$$

and

$$\hat{\tilde{K}}_{k,b}^* = \hat{\tilde{Y}}_{k,b}^*(U_k) - \hat{\tilde{P}}_{k,b}^*U_k = \frac{d\hat{\tilde{Y}}_{k,b}^*(U)}{d\hat{\tilde{Y}}_{k,b}^T(U)}\hat{\tilde{K}}_{k,b}.$$

C. Data-Driven TILC Broiler FCR Minimization

The objective is to minimize the terminal broiler FCR, which is unknown in broiler production. One reason for this is that artificial genetic selection progressively increases the growth rate. To account for this, the reference is redefined as

$$\tilde{R}_k^* = \tilde{Y}_k^*(U_k) - \mathcal{R} \tag{25}$$

where $\mathcal{R} \in \mathbb{R}_+^{N_y}$ is a trial-independent minimization vector with positive elements and this method is termed minimizing reference. As $\tilde{E}_k^*(U_k) = \tilde{R}_k^* - \tilde{Y}_k^*(U_k) = -\mathcal{R}$ is constant, zero tracking error is not possible by construction. Assuming that $\tilde{Y}_k^*(U_k)$ is lower bounded by $\tilde{Y}_{\min}^* \in \mathbb{R}^{N_y}$ and in combination with Theorem 2, the aim is to achieve

$$\lim_{k\to\infty} \tilde{Y}_k^*(U_k) = \tilde{Y}_{\min}^* \text{ and } \lim_{k\to\infty} \tilde{R}_k^* = \tilde{Y}_{\min}^* - \mathcal{R}. \tag{26}$$

Since broiler growth is a nonlinear process, a local minimum could be obtained instead of $\tilde{Y}_{\min}^*$.

In the following, the so-called best recent trial index κ_k is required, and for $\tilde{Y}_i^*(U_i) \in \mathbb{R}_+$, it is defined by

$$\kappa_k = \underset{i \in [\min(k-N_b,0),\, k]}{\arg\min} \left\|\tilde{Y}_i^*(U_i)\right\|_{W_{\tilde{E}}} \tag{27}$$

and serves as a feasible substitute for the best recent trial index given by

$$\underset{i \in [\min(k-N_b,0),\, k]}{\arg\min} \left\|\tilde{Y}_{\min}^* - \tilde{Y}_i^*(U_i)\right\|_{W_{\tilde{E}}}.$$

The variable i is lower bounded by 0, which equals the most recent preliminary trial and (27) is application-dependent. To reduce the influence of the measurement weight bias on κ_k, the slaughter weight Γ_k and the measured cumulative feed consumption $\tilde{Y}_{k,f}(U_k)$ are used

$$\kappa_k = \underset{i \in [\min(k-N_b,0),\, k]}{\arg\min} \left\|\frac{\tilde{Y}_{i,f}(U_i)}{\Gamma_i}\right\|_{W_{\tilde{E}}}. \tag{28}$$

To account for the uncertain nature of the augmented data-driven model given by (24), the TILC algorithm is modified into a descent type algorithm, denoted anchoring, by solving

$$U_{k+1} = \underset{U \in \Omega_{k+1}}{\arg\min} \left\|\tilde{E}_{\kappa_k}^*(U)\right\|_{W_{\tilde{E}}}^2 + \|U - U_{\kappa_k}\|_{W_{\Delta U}}^2 \tag{29a}$$

subject to (25), (28), and

$$\tilde{E}_{\kappa_k}^*(U) = \tilde{R}_{\kappa_k}^* - \tilde{Y}_{\kappa_k}^*(U) \tag{29b}$$

and

$$\tilde{Y}_{\kappa_k}^*(U) = \hat{\tilde{P}}_{k,\kappa_k}^*U + \hat{\tilde{K}}_{k,\kappa_k}^* \tag{29c}$$

where $\Omega_{k+1} \in \mathbb{R}^{N_u N_n}$ is the set of valid trial-dependent inputs.

Remark 1: The primary requirement for the algorithm outlined in this section to work in practice is that $\hat{\tilde{P}}_{k,\kappa_k}^*$ approximates $\tilde{P}_k^*$.

The input U_{k+1} is rejected if it does not decrease the error in (28) and U_κ is used instead of U_{k+1} in the next trial. This effectively ensures that the algorithm keeps exploring the neighborhood of the recent best trial input U_{κ_k} until the data-driven model is sufficiently accurate to maximize the terminal output norm in (28), as the data-driven model always uses the most recent data from the last N_b trials. Consequently, the data-driven model $\hat{\tilde{P}}_{k,\kappa_k}^*$ is identical to the analytical model $\tilde{P}_{\kappa_k}^*$ under ideal conditions and constant reference. In this case, $\kappa_k = k$ as $\tilde{E}_k^*$ is monotonically decreasing in k.

Remark 2: The convergence provided by Theorem 2 can no longer be guaranteed with the use of a data-driven model, as the associated optimization problem is no longer guaranteed to be convex.

This article has been accepted for inclusion in a future issue of this journal. Content is final as presented, with the exception of pagination.

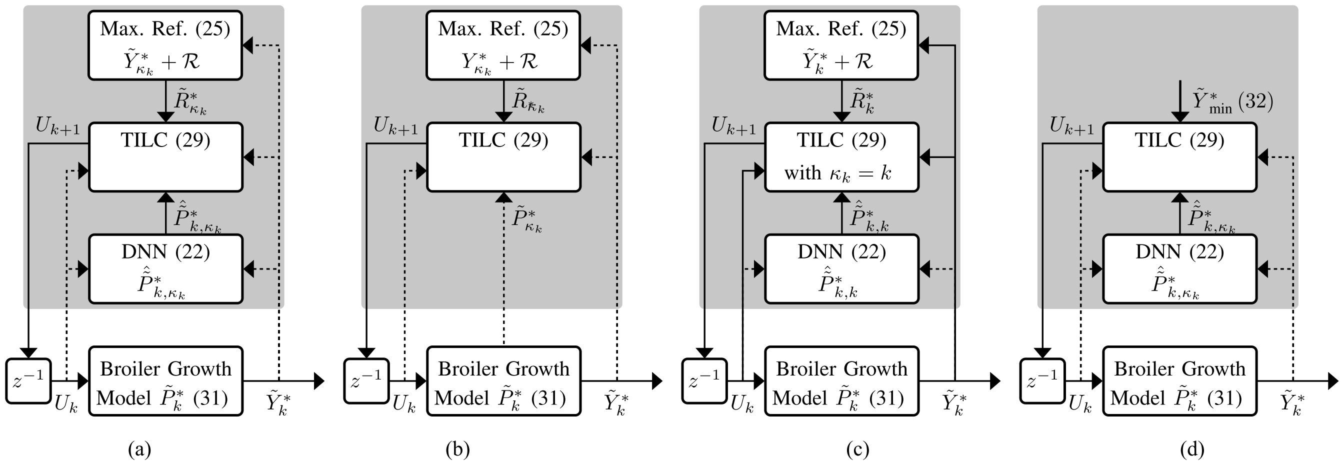

Fig. 9. Illustration of some of the configurations of the broiler growth optimization algorithm tested in Section IV. The shaded area denotes the controller, z^{-1} denotes a unit delay, a dashed signal contains information from the last N_b trials, $\{k-N_b+1, \ldots, k\}$, and a nondashed signal only contains information from trial k (see SectionIV-A for detailed explanation). (a) D + A + MR (Nominal). (b) I + A + MR (Without D). (c) D + MR (Without A). (d) D + A (Without MR).

The computable solution of (29) is

$$U_{k+1} = U_{\kappa_k} + \underset{\Delta U \in \Omega_{k+1} - U_{\kappa_k}}{\arg\min} \ \frac{1}{2}\|\Delta U\|^2_{Q_1} + Q_2^T \Delta U \quad (30)$$

where

$$Q_1 = 2\big(\hat{\tilde{P}}^{*T}_{k,\kappa_k} W_{\tilde{E}} \hat{\tilde{P}}^{*}_{k,\kappa_k} + W_{\Delta U}\big)$$

and

$$Q_2 = -2\hat{\tilde{P}}^{*T}_{k,\kappa_k} W_{\tilde{E}} \tilde{E}^*_{\kappa_k}(U_{\kappa_k})$$

and $\Delta U = U - U_{\kappa_k}$ results in an algorithm of the form $U_{k+1} = F(U_{\kappa_k}, \tilde{E}^*_{\kappa_k}(U_{\kappa_k})) = F(U_{\kappa_k}, \tilde{R}^*_{\kappa_k} - \tilde{Y}^*_{\kappa_k}(U_{\kappa_k}))$ that includes feedback action though the measured terminal output via the terms $\tilde{Y}^*_{\kappa_k}(U_{\kappa_k})$ and $\hat{\tilde{P}}^*_{k,\kappa_k}$. The slaughter weight is used to calculate $\tilde{E}^*_{\kappa_k}(U_{\kappa_k})$, similar to (28), to reduce the influence of the weight measurement bias. If combined with maximizing reference, then $\tilde{E}^*_k(U_{\kappa_k}) = \mathcal{R}$ and $\tilde{Y}^*_{\kappa_k}(U_{\kappa_k})$ is only used indirectly through $\hat{\tilde{P}}^*_{k,\kappa_k}$. This problem can be solved using the standard quadratic programming solvers, e.g., MATLAB's `quadprog`.

D. Analytical Heuristic Model

To evaluate the ILC algorithm formulated in Section III-C in simulation, an analytical linear terminal supervector broiler growth model of $\tilde{Y}_k$ is required. This is obtained by linearizing (2) along the trajectory of $U_k \in \mathbb{R}^{N_u N_n}$ using the first-order Taylor expansion

$$\tilde{Y}_k(U) \approx \tilde{Y}_k(U_k) + \tilde{P}_k\,(U - U_k) = \tilde{P}_k U + \tilde{K}_k \qquad (31)$$

with

$$\tilde{P}_k = \left.\frac{d\,\tilde{Y}_k(U_k)}{d\,U_k^T}\right|_{U_k} \text{ and } \tilde{K}_k = \tilde{Y}_k(U_k) - \tilde{P}_k U_k$$

where $\tilde{P}_k \in \mathbb{R}^{N_y \times N_u N_n}$ is the terminal model matrix and $\tilde{K} \in \mathbb{R}^{N_y}$ is the terminal output constant vector unrelated to the input $U \in \mathbb{R}^{N_u N_n}$.

IV. Simulation Case Study

A. Description

The objective is to investigate the ability of different configurations of the data-driven optimization algorithm (29) to minimize the terminal FCR $\tilde{Y}^*_k$ of the heuristic broiler growth model given by (2). Specifically, the performance impact of the following is investigated.

1) Using the data-driven model $\hat{\tilde{P}}^*_{k,\kappa_k}$ for control synthesis from (22), denoted by (D), compared to the unrealistic option of using the analytical supervector model $\tilde{P}^*_{\kappa_k}$ for control synthesis from (31), denoted by (I), as shown in Fig. 9(b).
2) Using anchoring from (29) though κ_k from (28), denoted by (A), compared to disabling this term by forcing $\kappa_k = k$, denoted by $(\cdot)$, as shown in Fig. 9(c).
3) Using the maximizing reference (25), denoted by (MR), compared to unrealistic option of using the analytic maximum given by

$$\tilde{R}^*_k = \tilde{Y}_{\min} = \underset{\sim}{z}[N_e] \qquad (32)$$

denoted by $(\cdot)$, as shown in Fig. 9(d).

This results in a total of eight different test configurations, some of which are shown in Fig. 9. Each test is repeated ten times and the mean true terminal error $|\tilde{Y}_k - \tilde{R}_{\max}|$ is used for evaluation.

To investigate the necessity for iterative learning in this data-driven application, different values of $W_{\Delta U}$ are explored under unconstrained conditions, i.e., $\Omega_k = \mathbb{R}^{N_e N_u}$, e.g., using $W_{\Delta U} = 0$ with a perfect model under linear conditions results in instantaneous convergence in a single trial. Specifically, if $W_{\Delta U} = 0$ has instantaneous convergence with the D+A+MR algorithm compared to using $W_{\Delta U} > 0$, then there is no need for iterative learning.

B. Method and Model Configuration

The heuristic broiler growth model in Section II was simulated between the initial sample $N_s = 0$ and the terminal

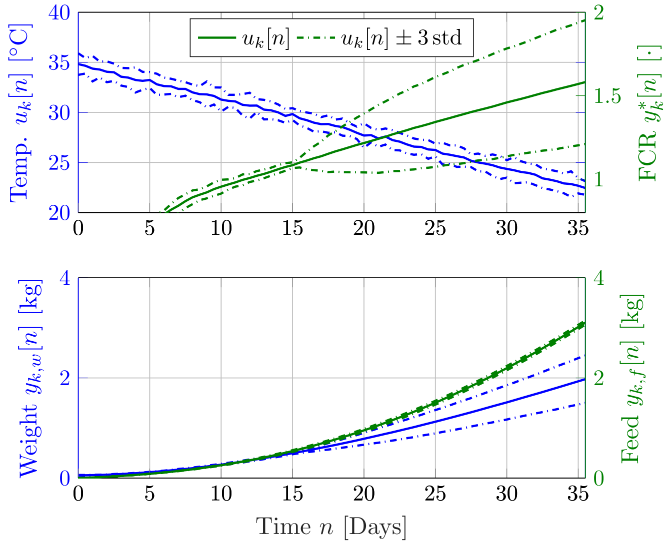

Fig. 10. Visualization of ten preliminary trial data. Note that the large FCR standard deviation is caused by the measured weight bias $q_{w,\text{bias}}[n]$.

sample $N_e = 35$ with a sample interval of $T_s = 0.5$ days and is heuristically configured with $\beta = 0.85$ as the worst case maturing rate, since feed and water consumption are the dominating factors and correct temperature control is regarded as a catalyst. Also, $\alpha = 0.05$ and $\sigma_u = 0.75$ [°C] have been used to give good overall sensitivity throughout the lifespan of a broiler.

The data-driven model in Section III-B is generated with $N_m = 20$ ensemble models using $N_b = 10$ preliminary training batches, $N_l = 3$ input and output lags, and $N_N = 7$ neurons in the hidden layer and with $N_S = 5$ initialization locations at samples $S = \{0, 7, 14, 21, 28\}$. The preliminary N_b trials required for training are generated using the positive input $u[n]$, resulting in a 5% decreased maturing rate, $G(u[n], x_m[n]) = 0.95$ (see the example in Fig. 10).

To ensure an identical initial input U_0 for all the tests, the most recent preliminary trial $k = 0$ does not have any added input noise. Hence, the objective is to decrease the terminal broiler FCR $\tilde{Y}_k^*$ by 0.0537. White noise with the standard deviation of 0.3 °C is added to the remaining $N_b - 1$ preliminary trials, $\{1 - N_b, \ldots, -1\}$. This is considered realistic, as most broiler farmers tend to use a too high temperature with little variations from trial-to-trial.

Fast convergence conditions for the data-driven TILC broiler optimization algorithm are obtained by using a minimization constant of $\mathcal{R} = 0.04$, terminal tracking error cost, and input change cost of $W_{\tilde{E}} = 0.01^{-2}$ and $W_{\Delta U} = \text{diag}([1\ \text{°C}]^{-2}, \ldots, [1\,\text{°C}]^{-2})$. The permitted temperature change is restricted to avoid large input fluctuations caused by data-driven modeling errors in $\hat{\tilde{P}}^*_{k,\kappa_k}$. The valid input space Ω_{k+1} is therefore given by

$$\omega_{k+1}[n] = \{u \mid -\gamma[n] \le u - u_{\kappa_k}[n] \le \gamma[n]\} \tag{33}$$

with

$$\gamma[n] = 0.5\ \text{°C} + n\,T_s\,\frac{1.5\ \text{°C}}{35\ \text{Days}}$$

TABLE I

Absolute FCR Error for the Different Model Configurations of the Last Trial ($k = 30$) of the Simulation Results in Fig. 11

Config.	FCR Error $[10^{-3}]$	Config.	FCR Error $[10^{-3}]$
I	1.4	D	60.3
I+A	1.4	D+A	19.6
I+MR	4.7	D+MR	51.1
I+MR+A	10.8	D+MR+A	24.2

where $u \in \mathbb{R}$ is the input and $\gamma[n]$ is the lower and upper temperature change bound ranging from 0.5 °C on day 0 to 2 °C on day 35. This does not restrict the permitted input space Ω_{k+1} for $k \to \infty$ as it changes with $u_{\kappa_k}[n]$.

C. Results

A summary of the simulation results is provided in Table I. From Fig. 11(a), it can be concluded that anchoring does not provide benefits under ideal modeling conditions, as I and I + A are almost identical—exactly as expected. However, anchoring is beneficial in conjunction with the data-driven model, as D fails to minimize FCR, while D + A converges, but significantly slower than, e.g., I. This makes anchoring superior under data-driven modeling conditions.

From I + MR in Fig. 11(b), it can be concluded that using maximizing reference produces similar results to the unrealistic case where the smallest possible FCR is known. Also, MR does not improve the convergence conditions with a data-driven model, since D + MR and D do not converge to zero error.

Using both MR and A, as shown in Fig. 11(c), leads to the conclusion that D + MR + A is the best performing implementable configuration of the algorithm, as D does not converge despite I and I + MR + A having superior performance. The convergence difference between I and D + MR + A is significant and is most notably caused by the measured weight bias $q_{w,\text{bias}}[n]$. To demonstrate that this is the case, removing the bias results in Fig. 11(d) by enforcing $q_{w,\text{bias}}[n] = 0$ results in a slightly slower convergence rate compared to I and also a final FCR offset of ≈ 0.01.

In Fig. 11(e), the D + MR + A algorithm is shown with different input change costs $W_{\Delta U}$, which demonstrates that if $W_{\Delta U}$ is configured too low, then the algorithm does not converge. Moreover, it suggests that iterative learning is required to solve the data-driven FCR minimization problem and TILC provides one possible solution.

V. Experimental Study

The results in this section are from an experimental study undertaken in a state-of-the-art broiler house situated in Northern Denmark, also considered in [8] and [10]. Each batch approximately contains 40 000 ROSS 308 broilers and an average duration of 34 days. A single production run conducted between June 27 and August 30, 2018, is detailed in the following.

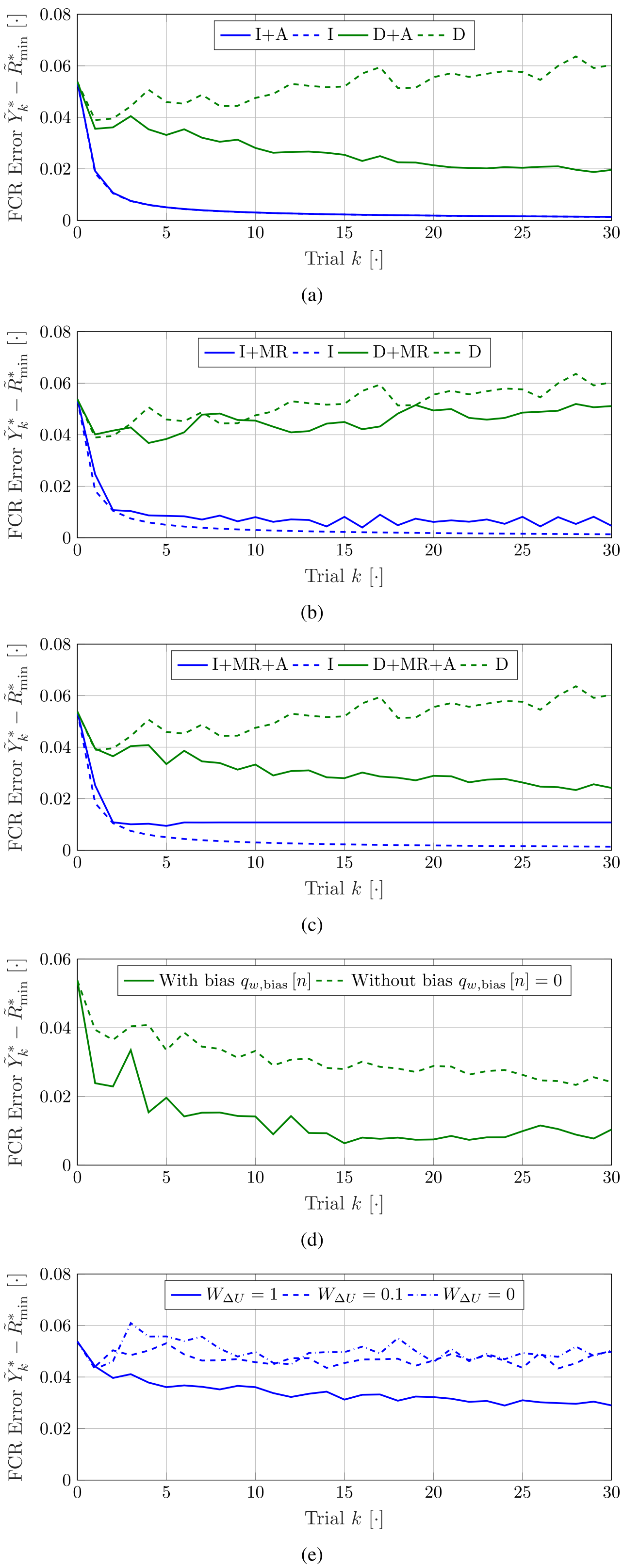

Fig. 11. Simulation results – see Section IV for detailed explanations. (a) Anchoring. (b) Maximizing Reference. (c) Anchoring and Maximizing Reference. (d) D + MR + A with and without weight measurement bias $q_{w,\text{bias}[n]} = 0$. (e) D + MR + A with different input change cost $W_{\Delta U}$ configurations.

A. Method Modification

This section details the modifications necessary for experimental testing of the D+A+MR algorithm developed in Section III-C.

1) Input Variable Selection: For detailed information concerning the input variable selection (IVS) algorithm, see [8]. State-of-the-art broiler production typically processes five–eight batches per house per year. The production parameters change over time as the broiler house deteriorates and both the broiler and feed performance increase. This effectively results in a parameter drift, which drastically reduces the amount of usable production data (although the parameter-drift rate has not yet been fully investigated). Furthermore, data quantity requirement scales exponentially with the number of inputs and input and output lags for the algorithm [8]. To alleviate this problem, mutual information-based IVS is used to select the most significant inputs, and input and output lags to make best use of the available production data.

The IVS is included by modifying the structure of $W^{\text{h}}_{u,i}$, $W^{\text{h}}_{y,i}$, and $W^{\text{h}}_{d,i}$. For example, if the disturbances indexed by 1 and 3 are selected with delay of $i = 2$, $N_d = 4$ disturbances, and $N_h = 3$ hidden neurons, then $W^{\text{h}}_{d,i}$ is

$$W^{\text{h}}_{d,2} = \begin{bmatrix} \mathcal{W}_1 & 0 & \mathcal{W}_2 & 0 \\ \mathcal{W}_3 & 0 & \mathcal{W}_4 & 0 \\ \mathcal{W}_5 & 0 & \mathcal{W}_6 & 0 \end{bmatrix}. \tag{34}$$

All inputs and outputs are not guaranteed to be present in all the available batches. To maximize the amount of available information, up to $N_b \in \mathbb{Z}_+$ potential batches are selected for the IVS algorithm by maximizing

$$\begin{aligned} \mathcal{B}_k = \arg\max_{\tilde{\mathcal{B}}} \; & N_{\tilde{d}}(\tilde{\mathcal{B}}) \cdot N_{\tilde{y}}(\tilde{\mathcal{B}}) \cdot \min\{\#\tilde{\mathcal{B}}, N_b\} \\ \text{s.t. } & \tilde{\mathcal{B}} \subseteq \{1 - N_{PB}, \ldots, k-1\} \end{aligned} \tag{35}$$

where $\mathcal{B}_k$ is the set of batches used for IVS and training on trial k, $\tilde{\mathcal{B}}$ is a set of potential batch indexes, N_b is the maximum number of batches considered, and $N_{\tilde{d}}(\tilde{\mathcal{B}})$ and $N_{\tilde{y}}(\tilde{\mathcal{B}})$ are the number of potential disturbances and outputs with batch indexes $\tilde{\mathcal{B}}$. Moreover, the temperature input, broiler weight output, and cumulative feed are required to form a potential batch.

2) Normalized FCR Cost Function: Batches have different durations, which makes FCR comparison difficult, and therefore, the FCR is normalized to the same weight ψ using the performance measure

$$J_{\text{FCR},\psi}(y_f, y_w) = \frac{y_f\left(1 - \frac{k_w}{\psi}\right) + y_w\left(\frac{k_f}{\psi}\right) - k_f}{y_w - k_w} \tag{36}$$

where $y_f \in \mathbb{R}_+$ is the average feed consumed per broiler, $y_w \in \mathbb{R}_+$ is the average slaughter weight, $\psi = 2.2$ kg, and $k_w = -1.110$ kg and $k_f = -3.081$ kg are correction factors. This cost function has been formulated using official regression formulas used by the Danish broiler industry [20, p. 85] and replaces the augmented data-driven model in (23) by

$$\tilde{Y}_k^*(U) = J_{\text{FCR},\psi}\big(\tilde{Y}_{k,f}(U), \tilde{Y}_{k,w}(U)\big). \tag{37}$$

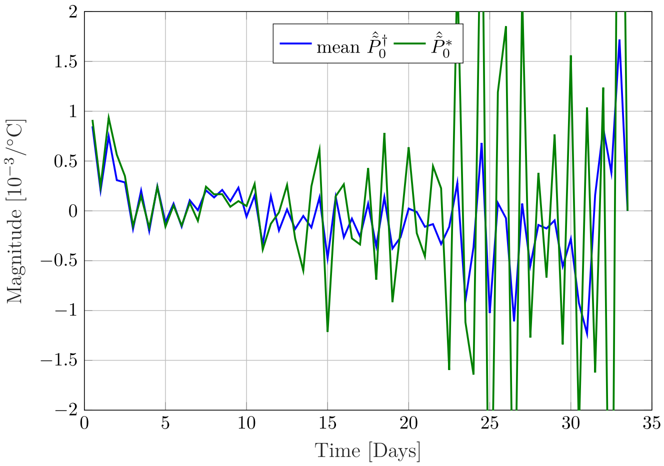

Fig. 12. $\hat{\hat{P}}_{k,\kappa_k}$ and the mean $\hat{\hat{P}}^\diamond_{k,\kappa_k}$ for $k = 0$ of the experimental test.

3) "Extended" TILC: In Fig. 12, the terminal system matrix $\hat{\hat{P}}^*_{k,\kappa_k}$ for $k = 0$ is shown, which has a significant degree of "ripple" from day 21 onward. This feature is caused by ripples in the training data and falsely suggests that FCR can be decreased by temperature fluctuations, as it results in either cold or heat stress. This promotes a loss of appetite and reduced growth during a period of desired maximum growth according to the FCR minimization considerations in Section II-B. A straightforward solution, available within point-to-point ILC framework, is to extend the terminal ILC design to include the last $N_\diamond \in \mathbb{Z}_+$ output samples, that is

$$Y_k^\diamond = \begin{bmatrix} y_k^*[N_e - N_\diamond + 1] & \cdots & y_k^*[N_e] \end{bmatrix}^T \in \mathbb{R}_+^{N_\diamond}. \quad (38)$$

The extended ILC problem now is

$$U_{k+1} = \underset{U \in \Omega_{k+1}}{\arg\min} \left\| \tilde{E}^\diamond_{\kappa_k}(U) \right\|^2_{W^\diamond_{\tilde{E}}} + \| U - U_{\kappa_k} \|^2_{W_{\Delta U}} \quad (39a)$$

subject to (28)

$$\tilde{R}_k^\diamond = \tilde{Y}_k^\diamond(U_k) - \mathcal{R}^\diamond \quad (39b)$$

$$\tilde{E}^\diamond_{\kappa_k}(U) = \tilde{R}^\diamond_{\kappa_k} - \tilde{Y}^\diamond_{\kappa_k}(U) \quad (39c)$$

and

$$\tilde{Y}^\diamond_{\kappa_k}(U) = \hat{\hat{P}}^\diamond_{k,\kappa_k} U + \hat{\hat{K}}^\diamond_{k,\kappa_k} \quad (39d)$$

where $W^\diamond_{\tilde{E}} \in \mathbb{R}^{N_\diamond \times N_\diamond}$, $\tilde{R}_k^\diamond \in \mathbb{R}^{N_\diamond}$, and $\hat{\hat{P}}^\diamond_{k,\kappa_k} \in \mathbb{R}^{N_\diamond \times N_\diamond}$. Note that (28) remains unchanged, and this approach is within the point-to-point ILC framework. Moreover, a high number of output samples $N_\diamond$ are undesirable, as it is equivalent to minimizing FCR over multiple days. This produces suboptimal results, as shown in Fig. 6.

B. Method Configuration

The IVS algorithm selects up to two variables from the available disturbances, e.g., CO2 denoted by $d_i[k \mid t]$ with index i, and up to two lags are selected per disturbance and input, e.g., $d_i[k-1 \mid t]$ and $d_i[k-3 \mid t]$. The weight shape cost function is configured with $N_\phi =$ day 15, and the extended TILC is configured with $N_\diamond = 4$ samples. A total of $N_m = 64$ ensemble models are used, of which the remaining settings are identical to the simulation study as described in Section IV-B.

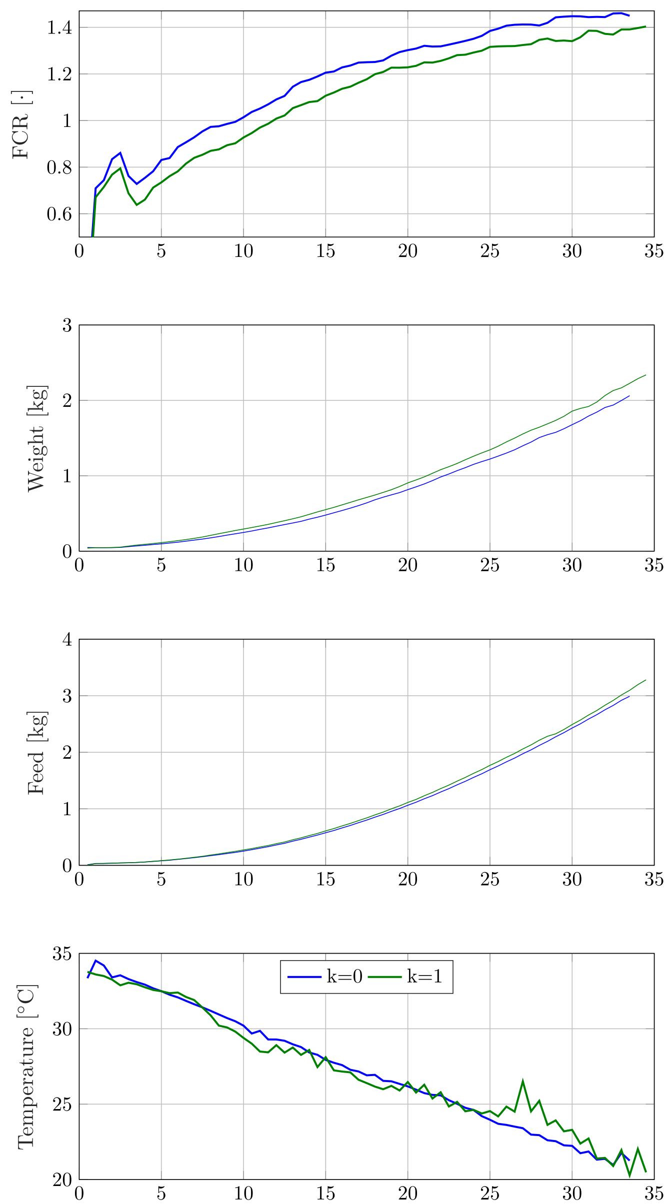

Fig. 13. Experimental results for $k = 1$ using the new design. The FCR, broiler weight, feed consumption, and measured temperature are shown for trial $k \in \{0, 1\}$ along with their difference in red. The temperature fluctuations from day 25 are caused by outside weather conditions and cannot be compensated for by the livestock stable climate control system.

C. Experimental Results

Fig. 13 shows the relevant measured signals for $k = 1$, where the FCR@2.2kg of trial $k = 1$ is approximately 6% smaller compared to $k = 0$. The terminal broiler weight is 200 g higher and the terminal cumulative feed consumption is only 100 g higher, which is a disproportionate exchange rate. The initial input change is approximately 0.5 °C lower for days 0–4 and 9–15 and approximately 2 °C higher for day 27. The initial decrease in temperature reduced the broiler growth rate, as the operator reported mild signs of cold stress in the broilers on visual inspection.

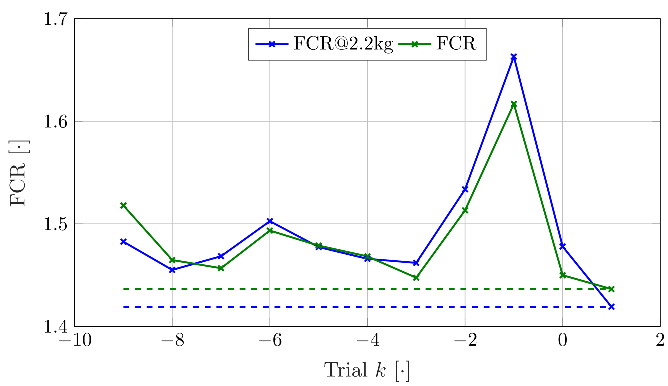

Fig. 14. FCR and FCR @ 2.2 kg performance overview of the recent ten trials $k \in \{-9, \ldots, 0\}$ and the current trial $k = 1$. Trial $k \in \{-2, -3\}$ have unusually high FCR due to an unusually cold winter, rendering the temperature regulation unable to maintain the desired temperature.

Applying the new design results in an FCR@2.2kg decrease of 5.9% (0.059) and an FCR decrease of 1.4% (0.014) for trial $k = 1$, calculated using the slaughter weight. In Fig. 14, the historic performance of the house is given, which shows that trial $k = 1$ has a very promising historically low FCR. This result is very close to the trial-to-trial FCR decrease for the first trial in the simulation study in Fig. 11 with an FCR decrease of approximately 1% (0.01).

These experimental results demonstrate the basic feasibility of the new design and provide a basis for onward development. A key outcome of these results is that data-driven models can give improvements on a trial-by-trial basis; however, the effects of anchoring require more trials for a comprehensive investigation. Especially considering that biological systems tend to be highly variable, short-term tests can sometimes give misleading results.

VI. Conclusion and Future Work

In this article, a heuristic broiler growth model has been formulated and used to investigate the performance of a data-driven FCR optimization-based ILC law in simulation and in practice. Traditional ILC is modified to minimize the terminal broiler FCR and to better cope with the uncertain nature of the data-driven model. The heuristic broiler growth model is based on the experience of a broiler application expert and approximates the dynamic behavior between broiler weight, feed uptake, and temperature, including a measurement weight bias commonly known to exist in the state-of-the-art broiler production. Extensive simulation-based studies confirm the potential of this approach, but the measurement weight bias is found to reduce the trial-to-trial convergence rate. The simulation study notably showed that iterative learning is required for FCR minimization.

Further modifications were made to prepare the algorithm for experimental testing in a real broiler house, and an FCR reduction of 1.4% was obtained over a single operation in a broiler house with around 40 000 broilers. It is worth noting that the broiler house used for the test documented in this article is among the best performing broiler producers in Denmark, and the potential FCR minimization potential of other producers could be expected to be even higher.

Possible areas for future research include studying the long-term properties of this design as briefly discussed in Section V and decreasing the effects of the measurement weight bias. Also, an investigation into whether or not the use of a rate of change constraint could reduce temperature fluctuations. Another area is to investigate if variance control could be used to increase flock uniformity and end product consistency.

References

[1] *OECD-FAO Agricultural Outlook 2018-2027*. OECD, Paris, France, Jul. 2018.

[2] D. A. Bristow, M. Tharayil, and A. G. Alleyne, “A survey of iterative learning control,” *IEEE Control Syst. Mag.*, vol. 26, no. 3, pp. 96–114, Jun. 2006.

[3] H.-S. Ahn, Y. Q. Chen, and K. L. Moore, “Iterative learning control: Brief survey and categorization,” *IEEE Trans. Syst., Man, Cybern. C, Appl. Rev.*, vol. 37, no. 6, pp. 1099–1121, Nov. 2007.

[4] I. Lim, D. J. Hoelzle, and K. L. Barton, “A multi-objective iterative learning control approach for additive manufacturing applications,” *Control Eng. Pract.*, vol. 64, no. 11, pp. 74–87, Jul. 2017.

[5] C. T. Freeman, E. Rogers, J. H. Burridge, A.-M. Hughes, and K. L. Meadmore, *Iterative Learning Control for Electrical Stimulation and Stroke Rehabilitation*. London, U.K.: Springer, 2015. [Online]. Available: https://www.springer.com/gp/book/9781447167259

[6] S. Haykin, *Neural Networks: A Comprehensive Found*. New York, NY, USA: MacMillan, 1994.

[7] S. V. Johansen, J. D. Bendtsen, M. Riisgaard-Jensen, and J. Mogensen, “Data driven broiler weight forecasting using dynamic neural network models,” *IFAC-PapersOnLine*, vol. 50, no. 1, pp. 5398–5403, Jul. 2017.

[8] S. V. Johansen, J. D. Bendtsen, M. Riisgaard-Jensen, and J. Mogensen, “Broiler weight forecasting using dynamic neural network models with input variable selection,” *J. Comput. Electron. Agricult.*, vol. 159, pp. 97–109, Apr. 2019.

[9] S. V. Johansen, M. R. Jensen, B. Chu, J. D. Bcndtsen, and E. Rogers, “Broiler growth optimization using norm optimal terminal iterative learning control,” in *Proc. IEEE Conf. Control Technol. Appl.*, Aug. 2018, pp. 1258–1264.

[10] S. V. Johansen, J. D. Bendtsen, and J. Mogensen, “Broiler slaughter weight forecasting using dynamic neural network models,” in *Proc. Int. Conf. Ind. Eng. Appl.*, Apr. 2019, pp. 463–470.

[11] Aviagen. (2010). *Environmental Management in the Broiler House*. [Online]. Available: http://en.aviagen.com/tech-center/download/236/Ross_Environmental_Management_in_the_Broiler_House.pdf

[12] Aviagen. (2014). *Ross 308 Broiler: Perform. Objectives*. [Online]. Available: http://en.aviagen.com/assets/Tech_Center/Ross_Broiler/Ross-308-Broiler-PO-2014-EN.pdf

[13] R. C. Newberry, J. R. Hunt, and E. E. Gardiner, “Behaviour of roaster chickens towards an automatic weighing perch,” *Brit. Poultry Sci.*, vol. 26, no. 2, pp. 229–237, Apr. 1985.

[14] A. Chedad, E. Vranken, J.-M. Aerts, and D. Berckmans, “Behaviour of chickens towards automatic weighing systems,” *IFAC Proc. Volumes*, vol. 33, no. 29, pp. 207–212, Nov. 2000.

[15] A. Chedad, J.-M. Aerts, E. Vranken, M. Lippens, J. Zoons, and D. Berckmans, “Do heavy broiler chickens visit automatic weighing systems less than lighter birds?” *Brit. Poultry Sci.*, vol. 44, no. 5, pp. 663–668, Dec. 2003.

[16] D. Prichard and J. Theiler, “Generating surrogate data for time series with several simultaneously measured variables,” *Phys. Rev. Lett.*, vol. 73, pp. 951–954, Aug. 1994.

[17] J.-X. Xu, Y. Chen, T. Lee, and S. Yamamoto, “Terminal iterative learning control with an application to RTPCVD thickness control,” *Automatica*, vol. 35, no. 9, pp. 1535–1542, 1999.

[18] B. Chu, C. T. Freeman, and D. H. Owens, “A novel design framework for point-to-point ILC using successive projection,” *IEEE Trans. Control Syst. Technol.*, vol. 23, no. 3, pp. 1156–1163, May 2015.

[19] S. V. Johansen, J. D. Bendtsen, and J. Mogensen, “Broiler growth optimization using optimal iterative learning control,” in *Proc. Amer. Control Conf.*, Jul. 2019, pp. 2203–2208.

[20] D. D. Fjerkæraad. (2013). *Årsberetning*.[Online]. Available: https://danskfjerkrae.dk/om-fjerkraebranchen/det-danske-fjaerkraeraad/aarsberetning/aarsberetning-2013

Simon V. Johansen received the M.S. degree in control engineering from Aalborg University, Aalborg, Denmark, in 2015. He is currently pursuing the Industrial Ph.D. degree in control engineering with Aalborg University and SKOV A/S, Roslev, Denmark.

His primary research interest is broiler feed efficiency optimization.

Martin R. Jensen completed his education as an Agricultural Technician and received the B.Com. degree in marketing from the Tietgen Business School, Odense, Denmark, and the B.Com. degree in financing from the Assens Business College, Glamsbjerg, Denmark, in 1994.

He is currently a Poultry Specialist with SKOV A/S, Roslev, Denmark. He is the owner of Mr Opti, Aalborg, Denmark, where he provides consulting services for poultry producers and integrators in Europe.

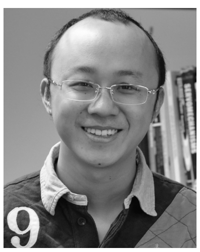

Bing Chu received the B.Eng. degree in automation and the M.Sc. degree in control science and technology from Tsinghua University, Beijing, China, in 2004 and 2007, respectively, and the Ph.D. degree in automatic control and systems engineering from The University of Sheffield, Sheffield, U.K., in 2009.

He was a Post-Doctoral Researcher with the University of Oxford, Oxford, U.K., from 2010 to 2012. He is currently an Associate Professor of electronics and computer science with the University of Southampton, Southampton, U.K. His current research interests include iterative learning and repetitive control, analysis and control of large-scale networked systems, applied optimization theory, and their applications to robotics, power electronics, and next-generation healthcare.

Dr. Chu was a recipient of a number of awards, including the Best Paper Prize of the 2012 United Kingdom Automatic Control Council International Conference on Control and the Certificate of Merit for the 2010 IET Control and Automation Doctoral Dissertation Prize.

Jan D. Bendtsen (M'11) was born in Denmark in 1972. He received the M.Sc.E.E. and Ph.D. degrees from the Department of Control Engineering, Aalborg University, Aalborg, Denmark, in 1996 and 1999, respectively.

Since 2003, he has been an Associate Professor with the Department of Electronic Systems, Aalborg University. In 2005, he was a Visiting Researcher with The Australian National University, Canberra, ACT, Australia. From 2012 to 2013, he was a Visiting Researcher with the University of California at San Diego, La Jolla, CA, USA. His current research interests include adaptive control of nonlinear systems, closed-loop system identification, control of distribution systems, and infinite-dimensional systems.

Dr. Bendtsen was a co-recipient of the Best Technical Paper Award at the AIAA Guidance, Navigation, and Control Conference in 2009. Since 2006, he has been on the organizing committee of several international conferences.

Jesper Mogensen received the B.A. degree in instrumentation and the Executive M.B.A. degree in technology management from Aalborg University, Aalborg, Denmark, in 1986 and 2013, respectively.

He has worked with management in the electronics industry for 25 years and is currently the Chief Technology Officer of SKOV A/S, Roslev, Denmark. His research interests include agile development, business development, and industry–university collaboration.

Eric Rogers is currently a Professor of control systems theory and design with the School of Electronics and Computer Science, University of Southampton, Southampton, U.K. His major research interests are in iterative learning control theory and applications in both engineering and healthcare, multidimensional systems theory and applications, long-range autonomy for autonomous underwater vehicles, and flow control.

Dr. Rogers is also the Editor-in-Chief of the *International Journal of Control and Multidimensional Systems* and *Signal Processing*. He has an extensive record of advisory work for funding agencies and industries in U.K. and elsewhere.